

See discussions, stats, and author profiles for this publication at: <https://www.researchgate.net/publication/231440361>

Role of Environmental Factors in the Dynamics of Intramolecular Dissociative Electron Transfer. Effect of Solvation and Ion-Pairing on Cleavage Rates of Anion Radicals

ARTICLE *in* JOURNAL OF THE AMERICAN CHEMICAL SOCIETY · SEPTEMBER 1995

Impact Factor: 12.11 · DOI: 10.1021/ja00141a028

CITATIONS

37

READS

26

3 AUTHORS, INCLUDING:



Claude Andrieux

Paris Diderot University

126 PUBLICATIONS 5,489 CITATIONS

SEE PROFILE



Marc Robert

Paris Diderot University

113 PUBLICATIONS 2,754 CITATIONS

SEE PROFILE

Role of Environmental Factors in the Dynamics of Intramolecular Dissociative Electron Transfer. Effect of Solvation and Ion-Pairing on Cleavage Rates of Anion Radicals

Claude P. Andrieux, Marc Robert, and Jean-Michel Saveant

J. Am. Chem. Soc., **1995**, 117 (36), 9340-9346 • DOI: 10.1021/ja00141a028

Downloaded from <http://pubs.acs.org> on January 15, 2009

More About This Article

The permalink <http://dx.doi.org/10.1021/ja00141a028> provides access to:

- Links to articles and content related to this article
- Copyright permission to reproduce figures and/or text from this article

Role of Environmental Factors in the Dynamics of Intramolecular Dissociative Electron Transfer. Effect of Solvation and Ion-Pairing on Cleavage Rates of Anion Radicals

Claude P. Andrieux, Marc Robert, and Jean-Michel Savéant*

Contribution from the Laboratoire d'Electrochimie Moléculaire de l'Université Denis Diderot, Unité Associée au CNRS No 438, 2 place Jussieu, 75251 Paris Cedex 05, France

Received April 27, 1995*

Abstract: Solvation and ion-pairing effects on the cleavage reactivity of anion radicals containing frangible bonds strongly depend upon the localization of the negative charge. When this is spread out over the entire molecular framework, as in haloanthracenes, the addition of water results in a small accelerating effect caused by specific solvation of the leaving anion. In anion radicals where the negative charge is concentrated on a small portion of the molecule, as on the oxygen atom of carbonyl or nitro groups, there is a considerable decrease of the cleavage reactivity upon addition of water. Stabilization of the leaving anion is still present, but it is largely overcompensated by a lowering of the energy of the orbital where the unpaired electron is located as revealed by a strong positive shift of the standard potential for the generation of the anion radical. The intramolecular electron transfer to the σ^* of the breaking bond thus possesses a lesser driving force. A change of mechanism ensues where cleavage is eventually replaced by $2e^- + 2H^+$ hydrogenation. For similar reasons, ion pairing agents, such as Li^+ or Mg^{2+} ions, have practically no effect on the cleavage rates and standard potentials of anion radicals with a largely delocalized negative charge, whereas strong effects are observed with anion radicals bearing a charge-localizing group, such as CO or NO_2 . The strong decrease in cleavage reactivity is again caused by the lowering of the energy well where the transferring electron sits. A change in mechanism also ensues where cleavage is eventually overrun by dimerization of the ion-paired radicals.

Coupling between electron transfer and bond dissociation (or bond formation) is one of the key problems in the comprehension of chemistry triggered by single electron transfer. This question indeed attracts continuous attention whatever the mode of electron injection involving direct or indirect electrochemistry,¹ pulse radiolysis,² and photochemistry.^{3,4} The distinction between concerted and sequential processes has now been firmly established on convergent experimental and theoretical grounds.^{1,5} The main molecular structure factors that govern the occurrence of one or the other mechanism have been identified.^{1,5} With concerted processes, application of a dissociative electron transfer Morse curve model has allowed the connection between

reaction dynamics and molecular structure factors such as homolytic bond dissociation energy and oxidation potential of the leaving group.^{1,5–7} Within sequential processes, the electron transfer step is of the outersphere type, and its dynamics may therefore be described by the Marcus–Hush model.⁸ The bond breaking step may be viewed as an intramolecular dissociative electron transfer and the reverse bond forming step as an intramolecular associative electron transfer. They may therefore be described by an extension of the dissociative electron transfer theory.^{1c,d,9} Here too, the predicted relationships between reactivity and molecular structure have received support from the available kinetic and reactivity trends data for bond cleavage in anion radicals as well as for coupling of radicals with nucleophiles, the two key steps of electron transfer stimulated reactions as, for example, $S_{RN}1$ substitutions.^{1c,d,9}

Solvation and ion-pairing effects on ion radical cleavage reactivity have so far received less attention than molecular structure effects. For dissociative electron transfer, the exact

* Abstract published in *Advance ACS Abstracts*, September 1, 1995.

(1) (a) Savéant, J.-M. Single Electron Transfer and Nucleophilic Substitution. In *Advances in Physical Organic Chemistry*; Bethel, D., Ed.; Academic Press: New York, 1990; Vol. 26, pp 1–130. (b) Savéant, J.-M. *Acc. Chem. Res.* **1993**, *26*, 455. (c) Savéant, J.-M. Dissociative Electron Transfer in *Advances in Electron Transfer Chemistry*; Mariano, P. S., Ed.; JAI Press: New York, 1994; Vol. 4, pp 53–116. (d) Savéant, J.-M. *Tetrahedron* **1994**, *50*, 10117.

(2) (a) Neta, P.; Behar, D. *J. Am. Chem. Soc.* **1980**, *102*, 4798. (b) Behar, D.; Neta, P. *J. Phys. Chem.* **1981**, *85*, 690. (c) Behar, D.; Neta, P. *J. Am. Chem. Soc.* **1981**, *103*, 103. (d) Behar, D.; Neta, P. *J. Am. Chem. Soc.* **1981**, *103*, 2280. (e) Bays, J. P.; Blumer, S. T.; Baral-Tosh, S.; Behar, D.; Neta, P. *J. Am. Chem. Soc.* **1983**, *105*, 320. (f) Norris, R. K.; Barker, S. D.; Neta, P. *J. Am. Chem. Soc.* **1984**, *106*, 3140. (g) Meot-Ner, M.; Neta, P.; Norris, R. K.; Wilson, K. *J. Phys. Chem.* **1986**, *90*, 168.

(3) (a) Saeva, F. D. *Topics Curr. Chem.* **1990**, *156*, 61. (b) Saeva, F. D. Intramolecular Photochemical Electron Transfer (PET)–Induced Bond Cleavage Reactions in some Sulfonium Salts Derivatives. In *Advances in Electron Transfer Chemistry*; Mariano, P. S., Ed.; JAI Press: New York, 1994; Vol. 4, pp 1–25.

(4) (a) Arnold, B. R.; Scaino, J. C.; McGimpsey, W. G. *J. Am. Chem. Soc.* **1992**, *114*, 9978. (b) Chen, L.; Farahat, M. S.; Gan, H.; Farid, S.; Whitten, D. G. *J. Am. Chem. Soc.*, in press.

(5) (a) Andrieux, C. P.; Le Gorande, A.; Savéant, J.-M. *J. Am. Chem. Soc.* **1992**, *114*, 6892. (b) Andrieux, C. P.; Differding, E.; Robert, M.; Savéant, J.-M. *J. Am. Chem. Soc.* **1993**, *115*, 6592. (c) Andrieux, C. P.; Robert, M.; Saeva, F. D.; Savéant, J.-M. *J. Am. Chem. Soc.* **1994**, *116*, 7864.

(6) (a) Savéant, J.-M. *J. Am. Chem. Soc.* **1987**, *109*, 6788. (b) Savéant, J.-M. *J. Am. Chem. Soc.* **1992**, *114*, 10595. (c) Bertran, J.; Gallardo, I.; Moreno, M.; Savéant, J.-M. *J. Am. Chem. Soc.* **1992**, *114*, 9576. (d) Lexa, D.; Savéant, J.-M.; Su, K. B.; Wang, D. L. *J. Am. Chem. Soc.* **1987**, *109*, 6464. (e) Lexa, D.; Savéant, J.-M.; Schäfer, H. J.; Su, K. B.; Vering, B.; Wang, D. L. *J. Am. Chem. Soc.* **1990**, *112*, 271. (f) Adcock, W.; Clark, C.; Houmam, A.; Krstic, A. R.; Pinson, J.; Savéant, J.-M.; Taylor, D. K.; Taylor, J. F. *J. Am. Chem. Soc.* **1994**, *116*, 4653.

(7) (a) Clark, K. B.; Wayner, D. D. M. *J. Am. Chem. Soc.* **1991**, *113*, 9363. (b) Huang, Y.; Wayner, D. D. M. *J. Am. Chem. Soc.* **1993**, *115*, 2157. (c) Workentin, M. S.; Maran, F.; Wayner, D. D. M. *J. Am. Chem. Soc.* **1995**, *117*, 2120.

(8) (a) Marcus, R. A. *J. Chem. Phys.* **1956**, *24*, 4966. (b) Hush, N. S. *J. Chem. Phys.* **1958**, *28*, 962. (c) Marcus, R. A. Theory and Applications of Electron Transfers at Electrodes and in Solution. In *Special Topics in Electrochemistry*; Rock, P. A., Ed.; Elsevier: New York, 1977; pp 161–179. (d) Marcus, R. A. *Faraday Discuss. Chem. Soc.* **1982**, *74*, 7. (e) Marcus, R. A.; Sutin, N. *Biophys. Biochim. Acta* **1985**, *811*, 265.

(9) Savéant, J.-M. *J. Phys. Chem.* **1994**, *98*, 3716.

evaluation of the solvent reorganization energy⁹ suffers the same degree of uncertainty as for outersphere electron transfer.¹⁰ It may be anticipated from some sparse available data that medium factors play an important role in governing the dichotomy between concerted and stepwise mechanisms. For example, there is a striking difference between the pulse radiolytic reduction of 3-cyanobenzyl bromide in water which was shown to follow a stepwise mechanism, even though the rate constant of the follow-up cleavage was too fast to be precisely measured,^{2c} and the electrochemical reduction of the same compound in acetonitrile that has been shown to follow a concerted mechanism.^{5a} This difference in behavior may be ascribed to two entirely different reasons. One is that the energy of the incoming electron is much larger in pulse radiolysis than in electrochemistry. The additional driving force thus offered in the first case may trigger a transition from a concerted to a stepwise mechanism. This effect of the energy of the incoming electron has recently been demonstrated in the electrochemical reduction of sulfonium cations^{5c} and of a vicinal dibromo compound.¹¹ However, the change of solvent from water to acetonitrile may as well be the cause of the change in mechanism.

In the work reported below, we have focused attention on solvation and ion-pairing effects on the dynamics of intramolecular dissociative electron transfer in the cleavage of anion radicals. From previous data one may note that cleavage of 4-nitrobenzyl chloride anion radical is 1000 times slower in water ($4 \times 10^3 \text{ s}^{-1}$)^{2a} than in acetonitrile ($4 \times 10^6 \text{ s}^{-1}$).^{5a} In other pulse radiolysis studies, cleavage rates of the anion radicals of 2-, 3-, and 4-chloroacetophenones, and 2-chlorobenzaldehyde,^{12a} 4-chlorobiphenyl, 1-chloronaphthalene, and 9-chloranthracene,^{12b} $\text{PhCO}(\text{CH}_2)_3 \text{X}$ ($\text{X} = \text{Cl}, \text{Br}, \text{I}$),^{12c} have been correlated with the electrophilic properties of the solvent (as measured by their Gutmann acceptor number). However the observed variations are small, 0.5–1 order of magnitude. Because of constraints imposed by the pulse radiolytic technique, the solvents (hexamethylphosphoric triamide, *N*-methyl-2-pyrrolidone, dimethylacetamide, *N,N*-dimethylformamide (DMF), dimethyl sulfoxide) cannot be too electrophilic and have therefore acceptor numbers that span no more than 5 units.¹³ In order to observe larger and more continuous variations of the reactivity, we have adopted a different strategy which consists in investigating the effect of progressive addition of water to acetonitrile or DMF.

The large effects thus observed and their interpretation have led us to anticipate likewise significant effects of ion-pairing on the cleavage rates of the same anion radicals. Large effects indeed appeared upon addition of Li^+ or Mg^{2+} ions to a DMF solution.

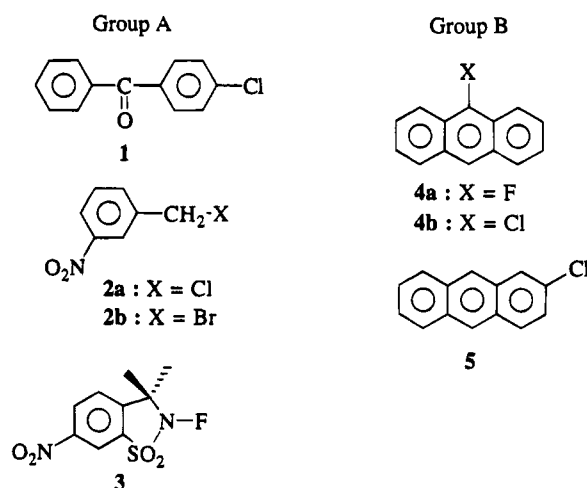
Another aspect of our strategy was also to contrast the behavior of two families of compounds (groups A and B) toward the addition of water and of Li^+ or Mg^{2+} . In group A, the negative charge is expected to be more localized (on the oxygen atoms of the CO or NO_2 groups) than in the anthracene derivatives in group B. The effects of solvation and ion-pairing are thus anticipated to be largely different in the two groups.

(10) (a) Fawcett, W. R.; Colby, A. F. *Electrochim. Acta* **1991**, *36*, 1767. (b) Fawcett, W. R.; Ferdusco, J. *Phys. Chem.* **1993**, *97*, 7075. (c) Grampp, G.; Jaenicke, W. *Ber. Bunsenges. Phys. Chem.* **1991**, *95*, 904.

(11) Andrieux, C. P.; Le Gorand, A.; Savéant, J.-M. *J. Electroanal. Chem.* **1994**, *377*, 191.

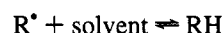
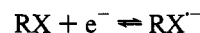
(12) (a) Kimura, N.; Takamaku, S. *Bull. Soc. Chim. Jpn.* **1986**, *59*, 3653. (b) Kimura, N.; Takamaku, S. *Radiat. Phys. Chem.* **1987**, *29*, 179. (c) Kimura, N.; Takamaku, S. *Bull. Soc. Chim. Jpn.* **1991**, *64*, 2433.

(13) (a) The cleavage rate of 9,10-dichloroanthracene anion radical was found to be the same in acetonitrile and in *N,N*-dimethylformamide.^{13b} However, the properties of these two solvents are again too similar for anticipating a significant variation of the reactivity. (b) Parker, V. D. *Acta Chem. Scand. B.* **1981**, *35*, 595.

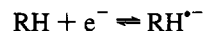


Results

Addition of Water. In the absence of water, **1** exhibits two cyclic voltammetric waves (Figure 1).¹⁴ The first one-electron irreversible wave corresponds to the reductive cleavage of the carbon–halogen bond according to the following reactions.



The benzophenone (RH) thus formed¹⁴ is reduced reversibly at the second wave into its anion radical



as checked with an authentic sample ($E^0 = -1.70 \text{ V}$ vs SCE). The formation of the halide ion ($\text{X}^- = \text{Cl}^-$) is attested by an irreversible anodic wave (1.09 V vs SCE at 0.5 V/s). Upon raising the scan rate, the first wave becomes reversible and then corresponds to the one-electron reversible formation of the anion radical. Simultaneously, the one-electron reversible reduction wave of benzophenone and the re-oxidation wave of Cl^- disappear, indicating that $\text{RX}^{\bullet-}$ is henceforth stable within the time scale of the experiment.

Addition of water, triggers a dramatic change in the cyclic voltammetric patterns. As seen, for example, in Figure 1, the addition of a water concentration of 0.58 M transforms the completely irreversible RX reduction wave at 0.2 V/s to a completely reversible wave at the same scan rate, thus pointing to a strong stabilization of the $\text{RX}^{\bullet-}$ anion radical.

As seen in Figure 2, **2a**^{5a} behaves in a very similar manner in the absence and presence of water, pointing again to a strong stabilization of the $\text{RX}^{\bullet-}$ anion radical caused by addition of water.

Similar phenomena were observed with **2b** although the cleavage of Br^- is faster than that of Cl^- in the absence^{5a} and presence of water. Analogous observations were made with **3**, which gives rise to a very fast cleaving anion radical.^{5b}

The variation of the cleavage rate constant¹⁵ with the concentration of water are represented in Figure 3 for all four compounds of group A. In all cases, we see that the cleavage rate constant decreases markedly as the water concentration is raised. For large water concentrations, the reaction rate starts to increase after passing through a minimum. This is represented on Figure 3 for **1** and was observed qualitatively for all other compounds. In this H_2O concentration range, the reduc-

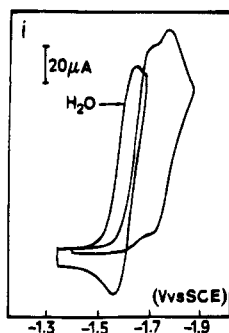


Figure 1. Cyclic voltammetry of **1** (2 mM) in $\text{CH}_3\text{CN} + 0.1 \text{ M } n\text{-Bu}_4\text{NBF}_4$ in the presence and absence of water (0.58 M). Scan rate: 0.2 V/s.

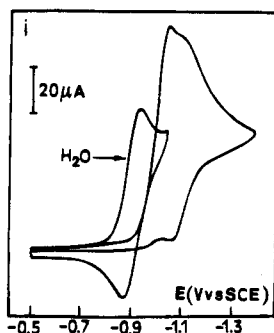


Figure 2. Cyclic voltammetry of **2a** (2 mM) in $\text{CH}_3\text{CN} + 0.1 \text{ M } n\text{-Bu}_4\text{NBF}_4$ in the presence and absence of water (2.6 M). Scan rate: 0.5 V/s.

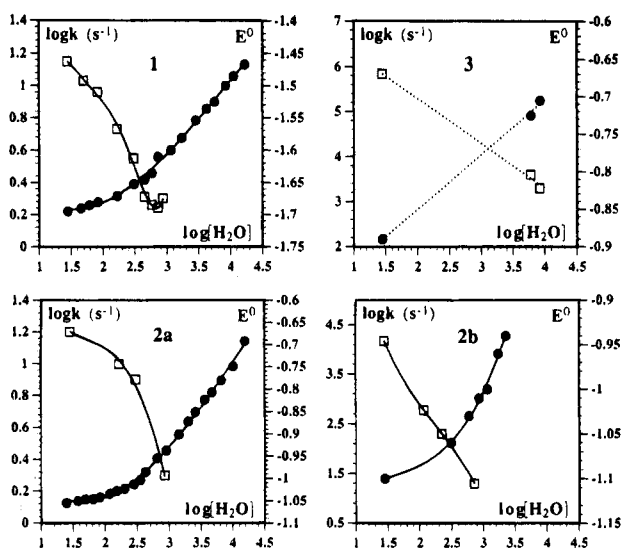
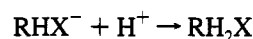
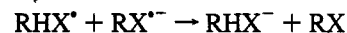
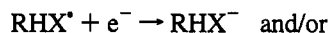


Figure 3. Variation of the cleavage rate constant and of the standard potential of the anion radical in compounds of group A in $\text{CH}_3\text{CN} + 0.1 \text{ M } n\text{-Bu}_4\text{NBF}_4$. $[\text{H}_2\text{O}]$ in mM and E^0 in V vs SCE.

tion wave of the corresponding dehalogenated compounds has become irreversible because of $2e^- + 2\text{H}^+$ hydrogenation. The

increase of the apparent rate constant thus indicates a change in the reaction mechanism where cleavage of the anion radical is replaced by its protonation and further reduction:



This conclusion is confirmed by the observation that, in this range of water concentrations, the anodic wave for the oxidation of the expelled Br^- or Cl^- ion tends to disappear.

For each concentration of water, the standard potential for the formation of the anion radical, E^0 , could be measured by raising the scan rate so as to obtain a reversible cyclic voltammogram. As seen in Figure 3, there is a large positive shift of E^0 upon increasing water concentration, which accompanies the decrease in cleavage rate constant. The same study was also carried out in DMF in the case of **1**. Very similar variations of the cleavage rate constant and of the standard potential with water concentration were found with only small changes in the absolute values. In all cases, the first point in the diagrams in Figure 3 as well as the starting voltammograms in Figures 1 or 2 correspond to acetonitrile solutions with no purposely added water. The residual water concentration was then 28 mM as determined by gas chromatography (see Experimental Section).

The compounds of group B were found to behave quite differently upon addition of water. In the absence of added water, their voltammograms exhibit a first irreversible wave followed by the two waves of anthracene (one reversible and the next one irreversible) as was checked from cyclic voltammetry of anthracene itself. Consistently, with **4b** and **5**, the oxidation wave of the Cl^- ion shows up upon scan reversal. The first wave of the halo-compounds could be made reversible by raising the scan rate, thus allowing the determination of the rate constant by which the initially formed radical disappears and of E^0 . Upon addition of water the same measurements could be made, but we also noted that the anthracene waves were always present after the first wave, even though the first of these tends to become irreversible as $[\text{H}_2\text{O}]$ increases. This observation shows that the irreversibility of the first wave of the halo-compounds is due to Cl^- expulsion and not to protonation of the anion radical. This is confirmed by the fact that, with **4b** and **5**, the Cl^- oxidation wave remains present when raising water concentration. The fact that in the same $[\text{H}_2\text{O}]$ range the first wave of anthracene itself is irreversible because of anion radical protonation indicates that the anion radicals of the halo-compounds are stabilized toward protonation by the presence of the halogen.

As seen in Figure 4, the cleavage rate constant¹⁵ now increases with water concentration, albeit to a modest extent, while the standard potential remains practically unaffected. The latter observation also applies to anthracene, while the protonation rate of its anion radical (represented together with the cleavage rate constant of the halo-compounds) increases steeply with $[\text{H}_2\text{O}]$.

(14) (a) Nadjo, L.; Savéant, J.-M. *J. Electroanal. Chem.* **1971**, *30*, 41. (b) The exact fate of R^{\bullet} depends upon the solvent used. In liquid NH_3 , a poor H-atom donor, R^{\bullet} is reduced immediately at the electrode or by the parent anion radical in solution giving rise to an overall two-electron process.^{14c} In acetonitrile the electron stoichiometry is 1. Analysis of electrolysis products, in DMSO, where the electron stoichiometry is also well below 2, showed the formation, besides benzophenone, of several products deriving from the same H-atom abstraction from solvent that yields benzophenone (aryl radicals are good H-atom scavengers).^{14d} For the present study, the only relevant point is that, in the absence of added water or of Li^+ or Mg^{2+} ions, the electron stoichiometry is 1. (c) Thiébaud, A.; Savéant, J.-M. *J. Electroanal. Chem.* **1978**, *89*, 335. (d) M'Halla, F.; Pinson, J.; Savéant, J.-M. *J. Electroanal. Chem.* **1978**, *89*, 347.

(15) The rate constants were derived from the anodic-to-cathodic peak current ratios using the integral equation appropriate for an "EC" mechanism.^{15b} Any finite difference simulation procedure could be used as well. (b) Andrieux, C. P.; Savéant, J.-M. *Electrochemical Reactions. In Investigations of Rates and Mechanisms of Reactions*; Bernasconi, C. F., Ed.; Wiley: New-York, 1986; Vol. 6, 4/E, Part 2, pp 305–390.

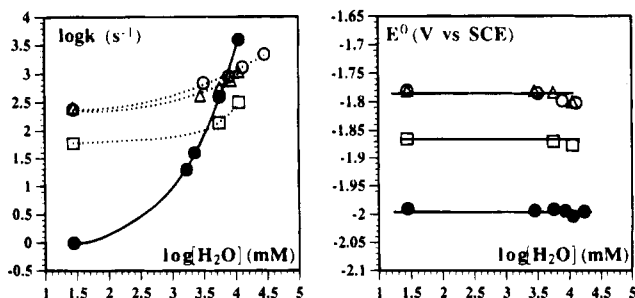


Figure 4. Variation of the cleavage rate constant and of the standard potential of the anion radical with water concentration in compounds of group B $CH_3CN + 0.1$ M $n\text{-Bu}_4\text{NBF}_4$. (○) 4a, (△) 4b, (□) 5, and (●) anthracene.

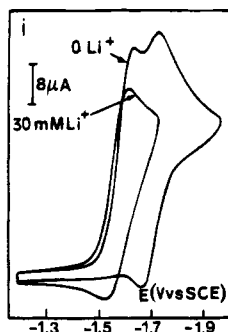


Figure 5. Cyclic voltammetry of 1 (1.86 mM) in DMF + 0.1 M $n\text{-Bu}_4\text{NBF}_4$ in the presence and absence of LiClO_4 . Scan rate: 0.5 V/s.

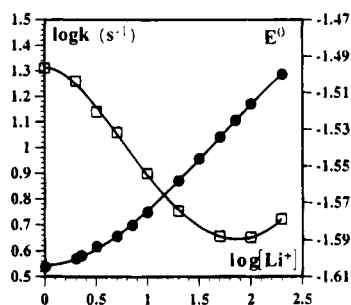


Figure 6. Variation of the cleavage rate constant and of the standard potential of the anion radical of 1 with Li^+ concentration (in mM) in DMF + 0.1 M $n\text{-Bu}_4\text{NBF}_4$. E^0 in V vs SCE.

Addition of Li^+ and Mg^{2+} . Figure 5 gives a typical example of the effect on the cyclic voltammogram of the addition of lithium cations to a DMF solution of 1 (DMF was preferred to acetonitrile in the study of ion-pairing because passivation of the electrode related to insolubility of intermediates occurred with the latter solvent). As with water, there is a steep decrease of the cleavage rate upon addition of Li^+ which renders the irreversible first wave of 1 at 0.5 V/s almost reversible for $[\text{Li}^+] = 30$ mM. The standard potential for the formation of the anion radical shifts positively upon addition of Li^+ . The variation of the cleavage rate constant¹⁵ and of E^0 with $[\text{Li}^+]$ are shown in Figure 6.

As with water addition, the apparent rate constant stops decreasing and starts then to increase, suggesting, here too, a change in mechanism in the process responsible for the irreversibility of the wave. This is confirmed by a closer examination of the whole wave system at high Li^+ concentrations (Figure 7). In the absence of Li^+ , benzophenone is produced at the first wave through cleavage of the C—Cl bond as attested by the presence, at more negative potentials, of its two waves, one reversible and one irreversible. The first, reversible, wave stands for the formation of the anion radical

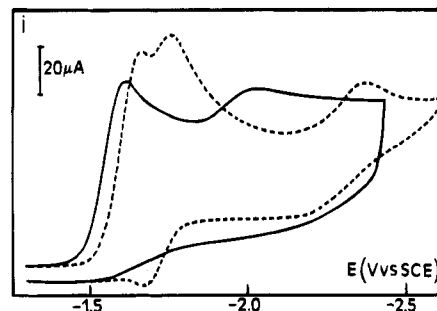


Figure 7. Cyclic voltammetry of 1 (1.87 mM) in DMF + 0.1 M $n\text{-Bu}_4\text{NBF}_4$ in the absence (—) and presence (—) of LiClO_4 (30 mM). Scan rate: 0.5 V/s.

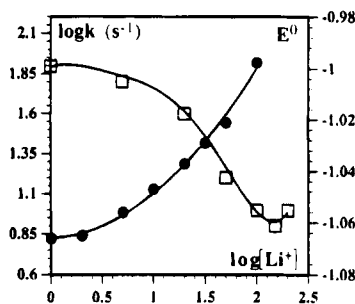


Figure 8. Variation of the cleavage rate constant and of the standard potential of the anion radical of 2a with Li^+ concentration (in mM) in DMF + 0.1 M $n\text{-Bu}_4\text{NBF}_4$. E^0 in V vs SCE.

(which is stable within the time scale corresponding to 0.5 V/s), and the second irreversible wave to its one-electron reduction coupled with protonation of the ensuing carbanion. In the presence of 30 mM Li^+ , the picture changes dramatically: the double-wave system disappears and is replaced by a small wave located in between the two waves of benzophenone. This small wave increases in height upon raising the scan rate as the first wave becomes reversible. The same picture is also obtained upon addition of Li^+ to a pure DMF solution of benzophenone. These observations are typical of the formation of a transient dimerizing radical as discussed previously,¹⁶ which, in the present case, results from ion-pairing of the initial anion radical followed by the reactions shown in Scheme 1. As a confirmation, we also noticed that the oxidation wave of Cl^- , observed in the absence of Li^+ , has now disappeared.

As seen in Figure 8, similar decrease of the cleavage rate constant¹⁵ and increase of the standard potential upon addition of Li^+ are also observed with another member of group A, 2a.

Conversely, in group B, addition of Li^+ has no noticeable effect either on the cleavage rate or on the standard potential, as checked in the case of 5.

We have also investigated the effect of adding magnesium ions. With 1, it was found that the interaction of the anion radical with Mg^{2+} ions is stronger than with Li^+ leading to the change of mechanism depicted in Scheme 1 at lower ion concentrations. As seen in Figure 9, the addition of substoichiometric amounts of Mg^{2+} triggers the appearance of a prewave governed by the diffusion of Mg^{2+} . This observation indicates that ion-pairing (Scheme 1) is much stronger than with Li^+ . In conditions where the prewave is seen, the main wave retains the same characteristics as in the absence of Mg^{2+} . Upon increasing the Mg^{2+} concentration, the prewave replaces completely the original wave, giving rise, as with Li^+ , to a wave system characteristic of the dimerization mechanism depicted in Scheme 1.

(16) (a) Andrieux, C. P.; Grzeszczuk, M.; Savéant, J.-M. *J. Am. Chem. Soc.* **1992**, *114*, 6892. (b) Andrieux, C. P.; Grzeszczuk, M.; Savéant, J.-M. *J. Electroanal. Chem.* **1991**, *318*, 369.

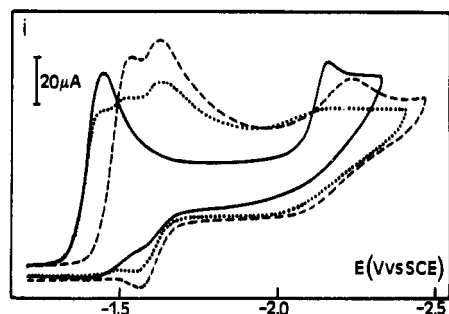
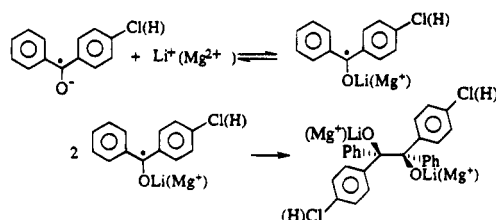


Figure 9. Cyclic voltammetry of **1** (1.85 mM) in DMF + 0.1 M $n\text{-Bu}_4\text{NBF}_4$ in the absence (—) and in the presence of 0.5 mM (···) and 1 mM (---) $\text{Mg}(\text{ClO}_4)_2$. Scan rate: 0.5 V/s.

Scheme 1



With **2a**, there is also a change in mechanism upon addition of a small amount of Mg^{2+} . As in the case of Li^+ and for the same reasons, the reaction that overruns cleavage is the reduction of the uncleaved anion radical caused by its interaction with Mg^{2+} , which, as in the case of **1**, is stronger with Mg^{2+} than with Li^+ .

Discussion

There is a striking difference between the variation of the cleavage reactivity of the anion radicals of groups A and B with addition of water, strong decrease for the first family and slight increase for the second. The same is true for the addition of ion pairing cations, Li^+ and Mg^{2+} . In both cases, the decrease of the cleavage reactivity parallels a positive shift of the standard potential of the $\text{RX}/\text{RX}^{\bullet-}$ couple.

The influence of the ion pairing cations is easier to rationalize than the influence of water in terms of molecule-to-molecule adduct. Scheme 2 summarizes the reaction mechanism in the case of **1**. The experimental data concerning Li^+ (Figures 6 and 8) are more amenable to quantitative analysis than those pertaining to Mg^{2+} because the change in mechanism is less abrupt, thus leaving room for a measurable observation of the cleavage reactivity decrease. The variation of the $\text{RX}/\text{RX}^{\bullet-}$ standard potential with the log of Li^+ concentration shows a linear section with a slope of 60 mV/unit on the right-hand side of the plot indicating, as represented in Scheme 2, the formation of a 1–1 $\text{RX}^{\bullet-}, \text{Li}^+$ adduct.¹⁷ Intersection of the horizontal and oblique straight lines leads to an association constant $K = 400 \text{ M}^{-1}$. From this, the standard potential of the $\text{RX}/\text{RX}^{\bullet-}, \text{Li}^+$ couple is found to be 160 mV more positive than that of $\text{RX}/\text{RX}^{\bullet-}$ couple.

The driving force of the cleavage reaction may be expressed as^{1c,d,9}

$$\Delta G_{\text{RX}^{\bullet-} \rightarrow \text{R}^{\bullet} + \text{X}^{\bullet-}}^0 = D_{\text{RX} \rightarrow \text{R}^{\bullet} + \text{X}^{\bullet-}} + E_{\text{RX}/\text{RX}^{\bullet-}}^0 - E_{\text{X}^{\bullet-}/\text{X}}^0 - T\Delta S \quad (1)$$

where D is the homolytic dissociation energy of the $\text{R}-\text{X}$ bond, the E^0 's, the standard potentials of the subscript couples, and $T\Delta S$ an entropic term. The bond dissociation energy is not expected to vary much from $\text{RX}^{\bullet-}$ to $\text{RX}^{\bullet-}, \text{Li}^+$. From the increase of the standard potential, the driving force should

therefore be 160 meV less favorable to cleavage in $\text{RX}^{\bullet-}, \text{Li}^+$ as compared to cleavage in $\text{RX}^{\bullet-}$. But what about a possible variation of the $E_{\text{X}^{\bullet-}/\text{X}}^0$ term? The answer is provided by the observation that the cleavage rate constant as well as $E_{\text{RX}/\text{RX}^{\bullet-}}^0$ do not vary appreciably upon addition of Li^+ ions in the case of 9-chloroanthracene. With this anion radical, the lack of variation of $E_{\text{RX}/\text{RX}^{\bullet-}}^0$ derives from the delocalization of the negative charge over the whole molecule. The lack of variation of the cleavage rate constant thus indicates that the $E_{\text{X}^{\bullet-}/\text{X}}^0$ is also insensitive to the presence of Li^+ ions in the concentration range of interest. Thus, in the case of **1**^{•−}, the decrease of the cleavage driving force can be estimated as 160 meV since it solely originates in the positive shift of $E_{\text{RX}/\text{RX}^{\bullet-}}^0$. In other words, the decrease of the cleavage driving force derives from a decrease of the π^* orbital energy upon formation of the $\text{RX}^{\bullet-}, \text{Li}^+$ adduct. What about the increase of the cleavage activation free energy? As shown earlier the activation free energy can be related to the driving force according to the following quadratic relationship:^{1c,d,9}

$$\Delta G_{\text{RX}^{\bullet-} \rightarrow \text{R}^{\bullet} + \text{X}^{\bullet-}}^{\ddagger} = \Delta G_{\text{RX}^{\bullet-} \rightarrow \text{R}^{\bullet} + \text{X}^{\bullet-}}^{\ddagger 0} \left(1 + \frac{\Delta G_{\text{RX}^{\bullet-} \rightarrow \text{R}^{\bullet} + \text{X}^{\bullet-}}^0}{4\Delta G_{\text{RX}^{\bullet-} \rightarrow \text{R}^{\bullet} + \text{X}^{\bullet-}}^{\ddagger 0}} \right)^2 \quad (2)$$

where the intrinsic barrier free energy, $\Delta G_{\text{RX}^{\bullet-} \rightarrow \text{R}^{\bullet} + \text{X}^{\bullet-}}^{\ddagger 0}$, can be expressed as

$$\Delta G_{\text{RX}^{\bullet-} \rightarrow \text{R}^{\bullet} + \text{X}^{\bullet-}}^{\ddagger 0} = \frac{D_{\text{RX} \rightarrow \text{R}^{\bullet} + \text{X}^{\bullet-}} + E_{\text{RX}/\text{RX}^{\bullet-}}^0 - E_{\text{R}^{\bullet}/(\text{R}^{\bullet})^{\bullet-}}^0 - T\Delta S^{\ddagger}}{4} \quad (3)$$

In the latter expression, $(\text{R}^{\bullet})^{\bullet-}$ derives from R^{\bullet} by injection of one electron in its π^* orbital. The variations of $E_{\text{RX}/\text{RX}^{\bullet-}}^0$ and $E_{\text{R}^{\bullet}/(\text{R}^{\bullet})^{\bullet-}}^0$ are likely to compensate each other because the degree of concentration of the negative charge on the oxygen atom should be about the same in both anions. It follows that the intrinsic barrier is unlikely to vary much upon interaction of the anion radical with Li^+ . On these grounds we may thus predict that the decrease of the cleavage activation free energy should be 80 meV, and therefore the decrease of the cleavage rate constant should be 20.

As the Li^+ concentration increases, the overall rate constant of cleavage derived from the cyclic voltammetric experiment should vary as

$$k_{\text{overall}} = \frac{k}{1 + K[\text{Li}^+]} + \frac{k'K[\text{Li}^+]}{1 + K[\text{Li}^+]}$$

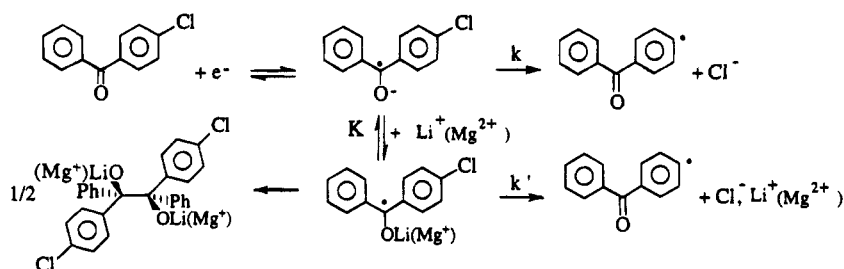
As $k'/k = 20$, there is no influence of the rate constant k' on the $\log k_{\text{overall}} - [\text{Li}^+]$ plot in the concentration range where the dimerization reaction has not yet overruled cleavage, meaning that the above equation reduces to

$$k_{\text{overall}} = \frac{k}{1 + K[\text{Li}^+]} \rightarrow \frac{k}{K[\text{Li}^+]} \quad \text{when } [\text{Li}^+] \gg 1/K$$

In the latter conditions, we thus expect that $\log k_{\text{overall}}/\log[\text{Li}^+] \rightarrow -1$. The fact that the absolute value of the experimental slope is smaller than 1 (Figure 6) reflects the increasing interference of the dimerization reaction which results in an increase of the apparent rate constant partially compensating the decrease of the cleavage reaction rate.

The results obtained with **2a**^{•−} (Figure 8) can be treated in the same manner. It is thus found that $K = 160 \text{ M}^{-1}$ and $E_{\text{RX}/\text{RX}^{\bullet-}, \text{Li}^+}^0 - E_{\text{RX}/\text{RX}^{\bullet-}}^0 = 130 \text{ mV}$. If the cleavage is under activation control as with **1**^{•−}, k/k' is predicted to be 13.

Scheme 2



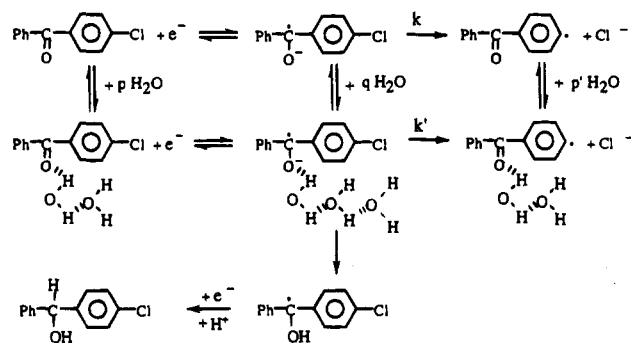
However, the cleavage intrinsic barriers for anion radicals of benzylic compounds are expected to be small, smaller than with aryl compounds, because the C—Br bond is weak. The reverse of the cleavage reaction may thus be a barrierless process in which case the log of the cleavage rate constant decreases proportionally to $\Delta G_{\text{RX}^{\cdot-} \rightarrow \text{R}^{\cdot} + \text{X}^-}$, i.e., faster than in the case of $1^{\cdot-}$. The ratio of the cleavage rate constants of $\text{RX}^{\cdot-}$ and $\text{RX}^{\cdot-}\text{Li}^+$ could thus be as large as 160. Another difference between $2\text{a}^{\cdot-}$ and $1^{\cdot-}$ is that the change in mechanism has less influence on the first part of the diagram leading to a slope of the $\log k_{\text{overall}}/\log[\text{Li}^+]$ line closer to unity.

The fact that the change in mechanism takes place earlier with Mg^{2+} than with Li^+ is the result of the stronger interaction of the former cation with the anion radical caused by its larger positive charge.

The influence of water can similarly be rationalized by examining its interactions with the species in the right-hand and left-hand members of the anion cleavage reaction. We first note that the E^0 of group B compounds is practically insensitive to water addition (Figure 4) as expected from the delocalization of the negative charge over the anthracene ring. At the upper end of the water concentration range E^0 decreases by a few millivolts. This small variation can be assigned to a change in the junction potential between the solution where water is added and the bridge connecting the cell to the aqueous SCE which has the same composition as the solution before addition of water.¹⁸ This observation indicates that we can safely neglect changes in the junction potential when examining the variations of E^0 upon addition of water with the group A compounds.

Another interesting observation is that the cleavage rate constant of the anion radicals in group B tends to increase upon addition of water in contrast with the decrease observed within group A. Among the various terms governing the cleavage driving force (eq 1), $E_{\text{RX}/\text{RX}^{\cdot-}}^0$ is insensitive to water addition as seen earlier but $E_{\text{X}^{\cdot-}/\text{X}^-}^0$ is expected to increase as a result of the stabilization of the halide ion. Since, the various terms in the intrinsic barrier are about constant, the increase in the cleavage rate constant results primarily from the increase of the $E_{\text{X}^{\cdot-}/\text{X}^-}^0$ term that decrease the standard free energy of reaction (in eq 1). We also note that the increase in the cleavage rate constant starts at relatively large concentrations of water (above 3 M), indicating that organization of large clusters of water molecules around the halide ion is necessary to promote its stabilization. This observation also indicates that with group A anion radicals, where most of the decrease of the cleavage rate occurs before 1 M water, the observed effect is essentially related to the positive shift of the $E_{\text{RX}/\text{RX}^{\cdot-}}^0$ term in the reaction standard free energy (eq 1) in the framework of the mechanism depicted in

Scheme 3



Scheme 3 with the example of compound 1 and which also applies to the nitro derivatives.

Unlike the case of Li^+ ions, the increase of E^0 upon addition of water does not reveal a clear molecule-to-molecule picture of the interaction between the anion radical and water molecules. The increase of E^0 is consistent with the progressive formation of a 1–2 adduct with $1^{\cdot-}$, and of a 1–3 adduct with $2\text{a}^{\cdot-}$ (Figure 3).¹⁹ Using either the 60 mV straight-line that may be drawn among the data points for $1^{\cdot-}$, or the 120 mV line that may be drawn at higher H_2O concentration, the increase in cleavage driving force is large enough in any case to entail a large decrease (larger than the factor of 20 found with Li^+ ions with $1^{\cdot-}$) of the cleavage rate constant upon specific solvation of the anion radical by water. The same conclusion applies to the other members of group A. The observed decrease of the apparent rate constant is therefore the result of a decrease of the relative concentration of the less water-solvated anion radicals as the water concentration increases. This interpretation has implicitly assumed that p , the number of water molecules possibly interacting with the oxygen atom in the anion radical precursor (Scheme 3), is zero. This is not necessarily true since the variations of E^0 merely measure the net solvation of $\text{RX}^{\cdot-}$ over RX . However, in such a case, the cause of the decrease of the cleavage rate constant would remain essentially the same since the interactions that contribute significantly to the decrease of the driving force involve the first few water molecules bound to the anion radical.

Conclusions

Solvation and ion-pairing effects on the cleavage reactivity of anion radicals containing a frangible bond strongly depends upon the localization of the negative charge. When this is spread out over the entire molecular framework, as in the haloanthracenes studied in this work, the addition of lithium or

(17) (a) Similarly to what has been previously observed with aromatic aldehydes and Na^+ or K^+ ions in the same solvent.^{17b} (b) Fawcett, W. R.; Lasia, A. *Canadian J. Chem.* **1981**, *59*, 3256.

(18) Addition of water is expected to stabilize the anion of the supporting electrolyte, BF_4^- , more than the cation $n\text{-Bu}_4\text{N}^+$ and thus to introduce a small Donnan potential difference at the junction (negative on the solution side, positive on the bridge side).

(19) (a) Previous studies of similar compounds not containing frangible bonds have indicated the formation of 1/1^{19b-d} and 1/2^{19c,d} adducts depending on the range of water concentration investigated and of the nature of the anion radical. (b) Svaan, M.; Parker, V. D. *Acta Chem. Scand. B* **1986**, *40*, 36. (c) Amatore, C.; Pinson, J.; Savéant, J.-M. *J. Electroanal. Chem.* **1982**, *139*, 193. (d) Genaro, A.; Romanin, A. M.; Severin, M. G.; Vianello, E. *J. Electroanal. Chem.* **1984**, *169*, 279.

magnesium ions has no effect on the cleavage rate, while addition of water results in accelerating effect at large water concentration caused by specific solvation of the leaving anion. In anion radicals where the negative charge is mostly concentrated on a small portion of the molecule, as on the oxygen atom of carbonyl or nitro groups, there is a considerable decrease of the cleavage reactivity upon addition of water. Stabilization of the leaving anion still exists, but it is largely overcompensated by a lowering of the energy of the orbital where the unpaired electron is located²⁰ as revealed by a strong positive shift of the standard potential for the generation of the anion radical. The intramolecular electron transfer to the σ^* of the breaking bond thus becomes slower because of a lesser driving force. The consequence is a change of mechanism where cleavage is eventually replaced by $2e^- + 2H^+$ hydrogenation as the water concentration is raised. For similar reasons, addition of ion pairing agents, such as Li^+ or Mg^{2+} ions, strongly decrease the cleavage reactivity of anion radicals bearing a charge-localizing group, such as CO or NO_2 . The strong decrease in cleavage reactivity is again caused by the lowering of the energy well where the transferring electron sits. A change in mechanism also ensues where, in this case, cleavage is eventually overrun by dimerization of the ion-paired radicals. The decrease of the cleavage reactivity can be correlated quantitatively with the parallel positive shift of the standard potential for the formation of the anion radical, as the result of a decrease of the free anion radical concentration upon addition of the ion pairing agent.

(20) The competition between these two opposing factors may be the cause for the variations of the cleavage reactivity observed by pulse radiolysis with the anion radicals of $PhCO(CH_2)_3$ or $4I$ (or Br or Cl) as a function of the acceptor properties of the solvent, decrease with the acceptor number for I, increase for Cl, and the passage through a minimum for Br.^{12c} However such pulse radiolysis experiments are not easy to interpret safely because the nature of counterions accompanying the generation of solvated electrons is usually unknown, and because their interaction with the anion radicals might be an important factor of cleavage reactivity.

(21) (a) Garreau, D.; Savéant, J.-M. *J. Electroanal. Chem.* **1972**, *35*, 309. (b) Garreau, D.; Hapiot, P.; Savéant, J.-M. *J. Electroanal. Chem.* **1989**, *272*, 1.

Experimental Section

Chemicals. Acetonitrile (Merck Uvasol), DMF (Burdick & Jackson), and the supporting electrolyte, $n\text{-Bu}_4\text{NBF}_4$ (Fluka, puriss), were used as received as well as **1**, **2a**, **2b**, **4a**, **4b** (Aldrich), and **5** (Janssen Chimica). **3** was prepared as described in ref 5b.

The concentration of residual water in acetonitrile was determined by gas phase chromatography with a Dils 30 instrument equipped with a 2 m Porapac Q column, a thermal conductivity detector and a Shimadzu integrator. The injection and detection temperature was 160 °C. We used the standard addition method whereby known amounts of water are added to acetonitrile and the residual water concentration is obtained from the intersection of the linear calibration line with the X axis. The concentration of residual water, 0.028 M, remained the same during three weeks after opening of the acetonitrile bottle. It was insensitive to the presence of the supporting electrolyte and to de-oxygenation of the solution by an argon stream. The concentration of water was calculated in each case from the measured actual volume of the water-acetonitrile mixture.

Instrumentation. Three different glassy carbon disk working electrodes were used in the standard cyclic voltammetry experiments according to the range of scan rates explored: a 3 mm diameter disk between 0.05 and 10 V/s, a 1 mm diameter disk between 5 and 100 V/s, and a 0.35 mm diameter disk between 50 and 1000 V/s. The first of these was built from a 3 mm diameter GC rod (from Tokai), the second from a 1 mm diameter rod obtained by mechanical abrasion of the original rod, and the third by sharpening the 1 mm diameter rod like a pencil. The GC pieces thus obtained were sealed inside a glass tube with epoxy resin. In the high scan rate experiments we used a 10 μm diameter carbon disk (Princeton Applied Research). The electrodes were carefully polished and ultrasonically rinsed with ethanol before each run. The counter electrode was a platinum wire, and the reference electrode was an aqueous SCE electrode.

The potentiostat, equipped with a positive feedback compensation and current measurer, used at low or moderate scan rates was the same as previously described.^{21a} The instrument used with ultramicroelectrodes at high scan rates has been described elsewhere.^{22b}

All experiments were carried out at 20 °C.

JA9513502